Experimental demonstration of a 25 GHz optoelectronic oscillator using an integrated resonant photoreceiver consisting of a GeSi photodiode and co-designed III-V low-noise amplifier

Vincent Crozatier
Thales Research & Technology
Palaiseau, France
vincent.crozatier@thalesgroup.com

Michiel Van Osta, Reinier Broucke, Laurens Bogaert, Joris Van Kerrebrouck, Nishant Singh, Guy Torfs
Ghent University – imec
Gent, Belgium
guy.torfs@ugent.be

2024 International Topical Meeting on Microwave Photonics (MWP) | 979-8-3503-7539-8/24/$31.00 ©2024 IEEE | DOI: 10.1109/MWP62612.2024.10736274

***Abstract*— We present an experimental demonstration of a 25 GHz optoelectronic oscillator made using an integrated resonant photoreceiver front-end. The front-end consists of an assembly with a photodiode and a co-designed low-noise amplifier that has an input network that provides optimum noise and power matching to the photodiode impedance. Due to the low noise figure and good power matching of the receiver front-end chipset, we measured a phase noise of -118 dBc/Hz @ 10 kHz offset and a floor of -154 dBc/Hz on a 5 dBm output tone.**

***Keywords*— optoelectronic oscillator, phase noise, microwave integrated circuits, photonic integrated circuits.**

I. Introduction

High frequency microwave signal generation using photonic architectures has been investigated for decades. Optoelectronic oscillators (OEO) are one example of such architectures [1]. OEOs rely on the low propagation loss of optical fibers to build a delay-line resonator, whose quality factor is proportional to the propagation time τ along the resonator. When carefully optimized, OEOs based on 1 km of optical fiber can offer ultra-low phase noise at 10 GHz [2]. Besides, the oscillation frequency is selected by a RF bandpass filter, among the resonance modes of the resonator, spaced by τ^{-1}. OEOs can directly generate high frequencies above the X band [3-5] up to W band [6], without frequency multiplication, thus with good efficiency. Further, the OEO oscillation signal is already modulated on an optical carrier making it ideal to distribute and synchronize local oscillator signals in distributed RADAR systems and high performance beyond 5G communication systems [7,8].

However, assembling an OEO is not as straightforward, as it consists in combining components, and choosing a relevant fiber length. Above 10 GHz, high performance optical and RF component become scarce. From that point of view, developing dedicated components is worth, especially considering the recent progress of photonic integrated circuits, and hybrid integration of RF dies on such circuits. OEwaves reported an impressive integrated OEO operating in Ka band, built around a lithium niobate whispering gallery mode resonator [9]. Yet, the packaged device consists off a manual assembly of different optical and RF parts.

As for the delay line, one usually implements very long optical fibers to improve close-to-carrier phase noise performances, at the expense of high spurious and possible instabilities. The fiber length can be tailored according to phase noise performance targets [2]. This optimization depends on the components used, especially the RF amplifiers additive phase noise (APN), while taking into account the fiber dispersion penalty when working at high RF frequencies [10].

In this paper, we investigate the performances of an OEO using a resonant photoreceiver operating at 25 GHz. Resonant photoreceivers implement a matching network between the photodiode and the amplifier and as such can simultaneously achieve high power gain and low noise figure. We measured the sensitivity and the APN of the receiver. We further implemented it in a direct 25 GHz OEO. We finally compare the OEO phase noise with simulations including the APN of the different devices.

II. Overview of the Resonant Photoreceiver and Additive Phase Noise Measurements

A photo of the assembled photoreceiver is shown in Fig. 1. It consists of a Ge-on-Si photodetector and co-designed GaAs low noise amplifier. The optical signal hits the photodiode through a grating coupler, which drops the intrinsic photodiode responsivity of 0.8 A/W at 1550 nm by 6 to 7 dB, depending on pigtail assembly. When supplied by 3 V, the amplification stage offers more than 24 dB gain, corresponding to a 224 V/W external conversion gain, over a 3-dB bandwidth between 23.5 and 31.5 GHz, ideally suited for 5G networks. The associated noise figure is 2.1 dB. The 1 dB compression point is reached for a 6 mW optical input power, while the output RF saturation level is 12 dBm.

This work was supported by the Horizon Europe project PATTERN with grant no. 101070506, the Special Research Fund of Ghent University (BOF) and the Flemish Research Counsel project no. G035722N.

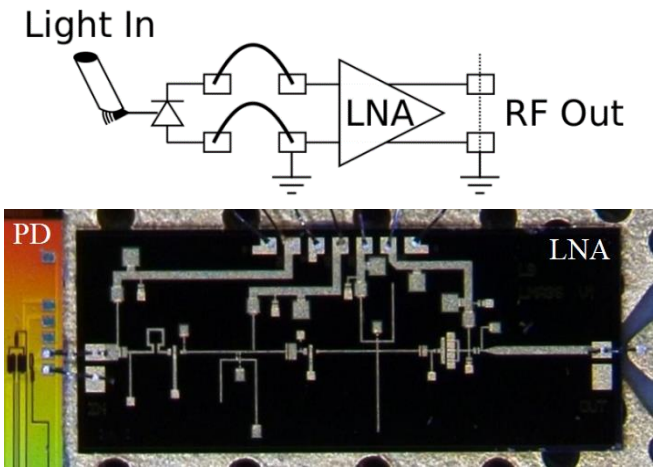

Fig. 1. Top: Schematic of the resonant photoreceiver showing photodiode (PD), low-noise amplifier (LNA) and RF wirebonds. Bottom: Image of the resonant photoreceiver assembly made using a silicon-photonics PD and a III-V LNA.

We measured the APN of the receiver, using the setup sketched in Fig. 2. We used a microwave photonic link built with a high power (100 mW) low noise distributed feedback (DFB) semiconductor laser, a low V_π (4.3 V at 25 GHz) Mach-Zehnder modulator (MZM) biased at quadrature, and a variable optical attenuator to set the optical power on the receiver close to the compression point. A low phase noise RF synthesizer (Rhode & Schwarz SMA100B) delivers a 25 GHz signal, which is used to drive the MZM (14 dBm) and down-converts the RF signal from the photoreceiver (typ. 3 dBm). We insert a phase shifter to set the RF double balanced mixer (Marki M9-0540) at quadrature. In this configuration, any voltage fluctuation from the mixer output is proportional to a phase fluctuation between the direct RF path and the mixed microwave photonic path. We use the baseband input of a Rhode & Schwarz FSWP-26 signal source analyzer to measure the voltage noise power spectral density (PSD), which is then calculated back into additive phase noise PSD of the photoreceiver.

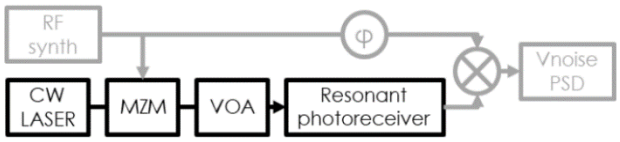

Fig. 2. Setup for receiver additive phase noise measurement. MZM: Mach-Zehnder modulator, VOA: variable optical attenuator. PSD: power spectral density. The black lines are optical signals while the grey lines are electrical signals.

Fig. 3 shows the results for two photoreceiver assemblies. They exhibit very similar performance, with a flicker part up to 10 kHz, followed by a noise floor level of -145 dBc/Hz, likely limited by the optical detection (shot-noise, noise figure of the photoreceiver and received signal power). We also performed APN measurement for a GaAs RF amplifier (Miteq JS4-26004000-27-10P), which has comparable gain (29 dB), noise figure (2.5 dB) and saturation output power (<17 dBm). We used the same setup as in Fig. 2, replacing the microwave photonic link with the sole RF amplifier. The results shown in Fig. 3 are obtained under linear and saturated regimes of the amplifier. One can observe that the low frequency part exhibits equivalent flicker levels. However, when the amplifier is saturated, the phase noise increases in the 1-100 kHz range. The steps on the curve stem from quantization of the FSWP input converter.

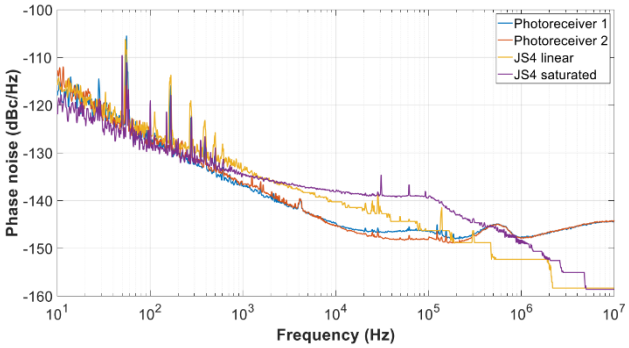

Fig. 3. Additive phase noise for two photoreceiver assemblies (blue and red), the RF amplifier in linear (yellow), and in saturation regime (purple).

III. Experimental Demonstration of a 25 GHz Optoelectronic Oscillator Using the Resonant Photoreceiver

In a second step, we assembled a single loop OEO around the photoreceiver as shown in Fig. 4. We used the same DFB laser and MZM as for the APN characterization. We built a basic RF bandpass filter (3 dB insertion loss) to provide sufficient frequency selectivity for the OEO to operate in a single frequency regime. From loop gain computation, it appeared that the overall gain is 7 dB lower than required to pass the oscillation threshold. We therefore added the RF amplifier after the filter. We also insert a 10 dB RF coupler after the photoreceiver. The coupled (-10 dB) output is sent to the OEO feedback path. With this setup, the OEO delivers more than 5 dBm at 25.4 GHz.

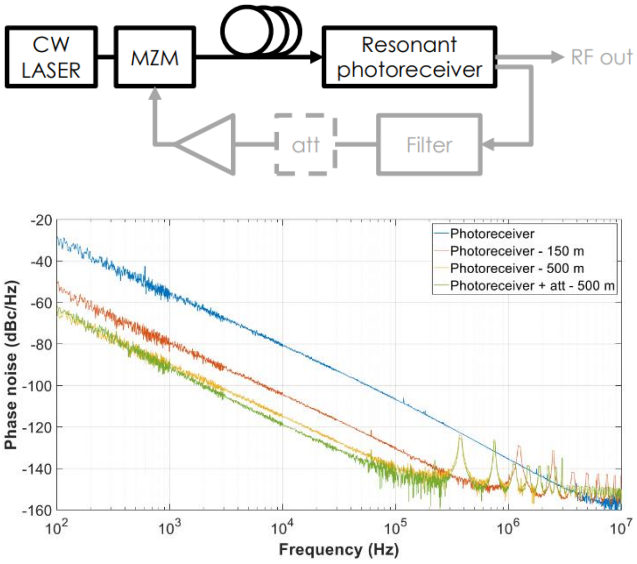

Fig. 4. Top: Overview of the optoelectronic oscillator made using a resonant photoreceiver. The black lines are optical signals while the grey lines are electrical signals. Bottom: Phase noise performances for 0 m (blue), 150 m (red) and 500 m (yellow) optical fiber. The green line includes 500 m of optical fiber and a 8 dB attenuator.

We recorded the OEO phase noise for different delay lines made of standard G.652 optical fiber (0 m, 150 m and 500 m) using the FSWP-26 signal source analyzer. Results are shown in Fig. 4. As the fiber gets longer, we observe a dramatic phase noise improvement. This is consistent with the increase of the quality factor of the resonator, which filters out the open-loop

phase noise contributions. We also notice that the spurious peaks corresponding to the non-oscillating modes get closer, which is consistent too. The peaks amplitude are attenuated by the FSWP measurement mode. It is worth noting that the phase noise measured with 150 m of fiber matches EVM requirements for 256 QAM [7].

In order to compare the performances with a standard OEO setup, we replaced the photoreceiver by a high-power broadband photodiode (0.55 A/W at 25 GHz, with a 50 Ohm resistive load), as shown in Fig. 5. We kept the same components, but used the RF coupler with the direct path to feed the filter and the amplifier. In this case, the available output power drops to -25 dBm. We also measured the phase noise with this configuration, using the same fiber lengths as shown in Fig. 5.

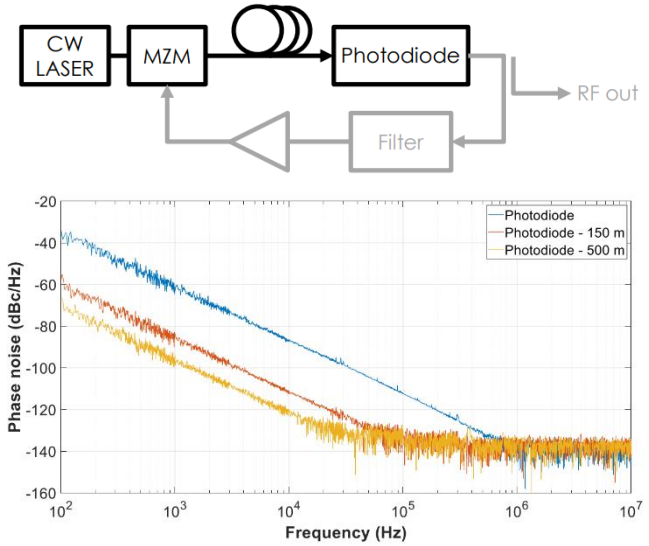

Fig. 5. Top: OEO setup with photodiode. The black lines are optical signals while the grey lines are electrical signals. Bottom: Phase noise performances for 0 m (blue), 150 m (red) and 500 m (yellow) delay line.

One can notice that for each fiber configuration, the OEO with the photoreceiver of Fig. 4 exhibits a 6 dB larger phase noise in the flicker region above 1 kHz, but a much lower noise floor. The former is induced by the larger power available at the measurement input. In the flicker part, the difference comes from the overall RF amplification APN. Indeed, in the configuration with the photoreceiver, one must consider both the photoreceiver and the RF amplifier APN. When using the standard photodiode, only the APN of the amplifier must be taken into account. Given the equivalent APN measured in Fig. 3, one should observe a 3 dB degradation of the phase noise. However, as the amplifier is likely to be saturated by the photoreceiver, the contribution from the amplifier may be larger.

We therefore measured the phase noise of the OEO with the photoreceiver including an 8 dB attenuation before the RF amplifier, to have equivalent RF power at the RF amplifier input with the case of the OEO with the standard photodiode. With a 500 m of fiber, one clearly observes that the phase noise is lower above 1 kHz offset frequency, which is consistent with the saturated behavior of the RF amplifier and indicates that the RF amplifier is limiting the performance.

IV. Simulation with Phase Noise Model

In order to assess this observation, we used a phase noise model to check for limitations of the performances of the assembled OEO [2], including the photoreceiver sensitivity, gain, noise figure, and the APN measured for the photoreceiver and the RF amplifier. Fig. 6 shows simulation results (dashed line) and experimental traces (solid lines, smoothed for reading) for each of the following OEO configurations including the 500 m delay line:

- standard photodiode;
- photoreceiver;
- photoreceiver and attenuator.

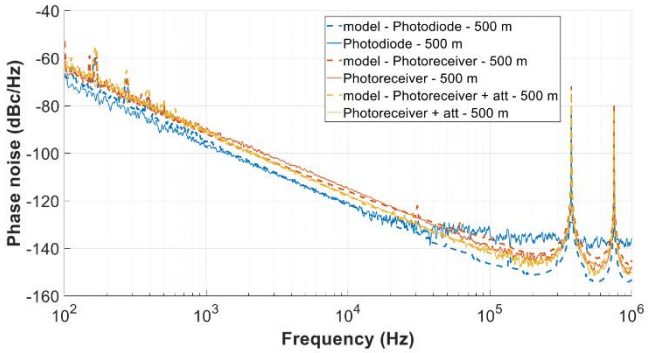

Fig. 6. Experimental (solid) and simulated (dashed) phase noise of the 500 m OEO using the photodiode (blue), the photoreceiver (red), and the photoreceiver with an attenuator (yellow).

We notice that the agreement is perfect for the photodiode OEO, and for the photoreceiver OEO including the attenuator. Without attenuator, one can observe a slight discrepancy, likely due to APN sensitivity to saturation, or coupling between amplitude noise and phase noise in our measurement. Although not shown here for sake of clarity, the agreement remains the same with shorter fiber lengths.

TABLE I. Comparison with some low phase noise OEOs directly oscillating in the 20 - 30 GHz range.

	Frequency (GHz)	**Phase noise @ 10 kHz (dBc/Hz)**	**Phase noise floor (dBc/Hz)**
This	25.4	-118	-154
[3]	3-28	-102	-138
[4]	30	-130	-138
[5]	20	-110	-

Tab. 1 compares the performance with respect to reported work of low phase noise OEOs directly oscillating in the 20-30 GHz range. Our architecture based on a resonant photoreceiver shows promising phase noise performances, which could be further optimized.

V. Conclusion

We have demonstrated a 25 GHz OEO built around a resonant photoreceiver. Thanks to the low noise figure and power matching of the photoreceiver, the OEO provides a 5 dBm output signal with a noise floor of -154 dBc/Hz. With 500 m of fiber, the phase noise is -118 dBc/Hz at 10 kHz offset frequency, limited by the APN of the photoreceiver and the amplifier.

References

[1] X. S. Yao and L. Maleki, “Converting light into spectrally pure microwave oscillation,” Opt. Lett., vol. 21, pp.483–485, April 1996.

[2] O. Lelièvre, V. Crozatier, P. Berger, G. Baili, O. Llopis, D. Dolfi, P. Nouchi, F. Goldfarb, F. Bretenaker, L. Morvan, and G. Pillet, “A model for designing ultralow noise single- and dual-Loop 10-GHz optoelectronic oscillators,” J. Lightw. Technol., vol. 35, pp. 4366–4374, October 2017.

[3] W. Li and J. Yao, “A wideband frequency tunable optoelectronic oscillator incorporating a tunable microwave photonic filter based on phase-modulation to intensity-modulation conversion using a phase-shifted fiber Bragg grating,” IEEE Trans. Microw. Theory Techn., vol. 60, pp. 1735–1742, March 2012.

[4] A. Ly, V. Auroux, R. Khayatzadeh, N. Gutierrez, A. Fernandez, and O. Llopis, “Highly spectrally pure 90-GHz signal synthesis using a coupled optoelectronic oscillator,” IEEE Photon. Technol. Lett., vol. 30, pp. 1313–1316, June 2018.

[5] S. Zhao and J. Yan, “Low phase noise optoelectronic oscillator based on an electroabsorption modulated laser,” Appl. Opt., vol. 58, pp. 4512–4517, June 2019.

[6] G. K. M. Hasanuzzaman, S. Iezekiel, and A. Kanno, “W-Band optoelectronic oscillator,” IEEE Phot. Techno. Lett., vol. 32, pp. 771–774, July 2020.

[7] F. Zou, L. Zou, B. Yang, Q. Ma, X. Zou, J. Zou, S. Chen, D. Milosevic, Z. Cao, and H. Liu, “Optoelectronic oscillator for 5G wireless networks and beyond,” J. Phys. D: Appl. Phys., vol. 54, p.423002, August 2021.

[8] A. Moerman, J. Van Kerrebrouck, O. Caytan, I. L. de Paula, L. Bogaert, G. Torfs, P. Demeester, H. Rogier, and S. Lemey, “Beyond 5G without obstacles: mmwave-over-fiber distributed antenna systems,” IEEE Communications Magazine, vol. 60, pp. 27–33, January 2022.

[9] L. Maleki, “The optoelectronic oscillator,” Nat. Photon., vol. 5, pp. 728–730, December 2011.

[10] D. Chang, H. Fetterman, H. Erlig, H. Zhang, A. Oh, C. Zhang, and W. Steier, “39-GHz optoelectronic oscillator using broad-band polymer electrooptic modulator,” IEEE Photon. Technol. Lett., vol. 14, pp. 191–193, February 2002.